The Role of the Mixed Layer in Setting the Potential Vorticity of the Main Thermocline

RICHARD G. WILLIAMS

Space and Atmospheric Physics Group, Department of Physics, Imperial College, London, United Kingdom

(Manuscript received 20 September 1990, in final form 26 April 1991)

ABSTRACT

A steady ventilation model is used to assess the effect of the mixed layer on the structure of the main thermocline; the potential vorticity is found in a subtropical gyre after imposing the thickness and density of the mixed layer, the Ekman pumping, and the hydrography on the eastern boundary.

The modeled potential vorticity becomes comparable in value to observations in the North Atlantic if the mixed layer deepens poleward as is observed in winter. The isopycnal gradients in potential vorticity are reduced on the denser ventilated surfaces if the mixed-layer outcrops deviate from latitude circles and, more realistically, sweep southward along the eastern boundary; the age of the subducted fluid is also in reasonable agreement with observations of the tritium–helium age by Jenkins.

This study suggests that ventilation may form much of the extensive region of nearly uniform potential vorticity observed on the $\sigma_\theta = 26.75$ surface in the North Atlantic, with lateral mixing by eddies being required only in the unventilated pool on the western side of the gyre.

1. Introduction

In attempting to understand the structure of the main thermocline of the ocean, the theoretical focus is on the large-scale potential vorticity field, Q,

$$Q = -\frac{f}{\bar{\rho}}\frac{\partial \rho}{\partial z} \tag{1}$$

and those processes that determine it. Here relative vorticity is neglected on the gyre scale; f is the planetary vorticity, z is the vertical coordinate, ρ is the density, and $\bar{\rho}$ is a reference density. Climatological maps of Q derived from large-scale hydrography show how the gyre circulation can be separated into regions of open, closed, and blocked Q contours; typical examples can be seen in McDowell et al. (1982) (shown in Fig. 1), Keffer (1985), and Stammer and Woods (1987).

Ventilation occurs on the open Q contours that thread back to the sea surface, where the Q is set when fluid is subducted from the mixed layer (Luyten et al. 1983). In contrast, homogenization tends to occur within closed Q contours by way of synoptic-scale eddies transferring Q downgradient from a uniform value on a bounding streamline (Rhines and Young 1982). For example, in the North Atlantic, the open Q contours on the $\sigma_\theta = 26.4$ surface are usually associated with ventilation, whereas the nearly uniform Q field on the $\sigma_\theta = 26.75$ surface is associated with homogenization by eddies (Fig. 1). While homogenization is probably important in the eddy-rich Gulf Stream recirculation (Marshall and Nurser 1986), we investigate here whether ventilation might instead form the nearly uniform Q extending over the rest of the gyre.

Indeed, in contrast to the Q observations, the corresponding tritium–helium age distributions from Jenkins (1988) show a similar overall pattern to each other (Fig. 2) and appear consistent with the ventilated picture of fluid being subducted in the northeast Atlantic, and increasing in age while following the anticyclonic circulation of the gyre. It is possible that ventilation and homogenization might produce similar age fields, but with very different Q fields, given the appropriate eddy diffusion and boundary conditions. However, we feel that scenario is unlikely and instead examine the alternative hypothesis that ventilation actually controls both Q and age distributions over much of the subtropical gyre.

In this paper we discuss the role of the mixed layer in setting the potential vorticity of subducted fluid (section 2) and then use a steady ventilation model for an idealized study of the subtropical gyre (section 3). We concentrate on how the subducted Q field is influenced by the slope and outcrop geometry of the winter mixed layer (section 4) following the ideas of Stommel (1979), who argues that the end of winter is the most crucial time for ventilating the main thermocline, and Woods (1985), who emphasizes the importance of the lateral transfer of fluid from a sloping mixed layer into the thermocline. This extends the variable mixed-layer depth studies of Williams (1989) and Pedlosky and Robbins (1991), while it is more idealized than the

Corresponding author address: Dr. R. G. Williams, Department of Earth, Atmospheric, and Planetary Sciences, Rm. 54-1412, MIT, Cambridge, MA 02139

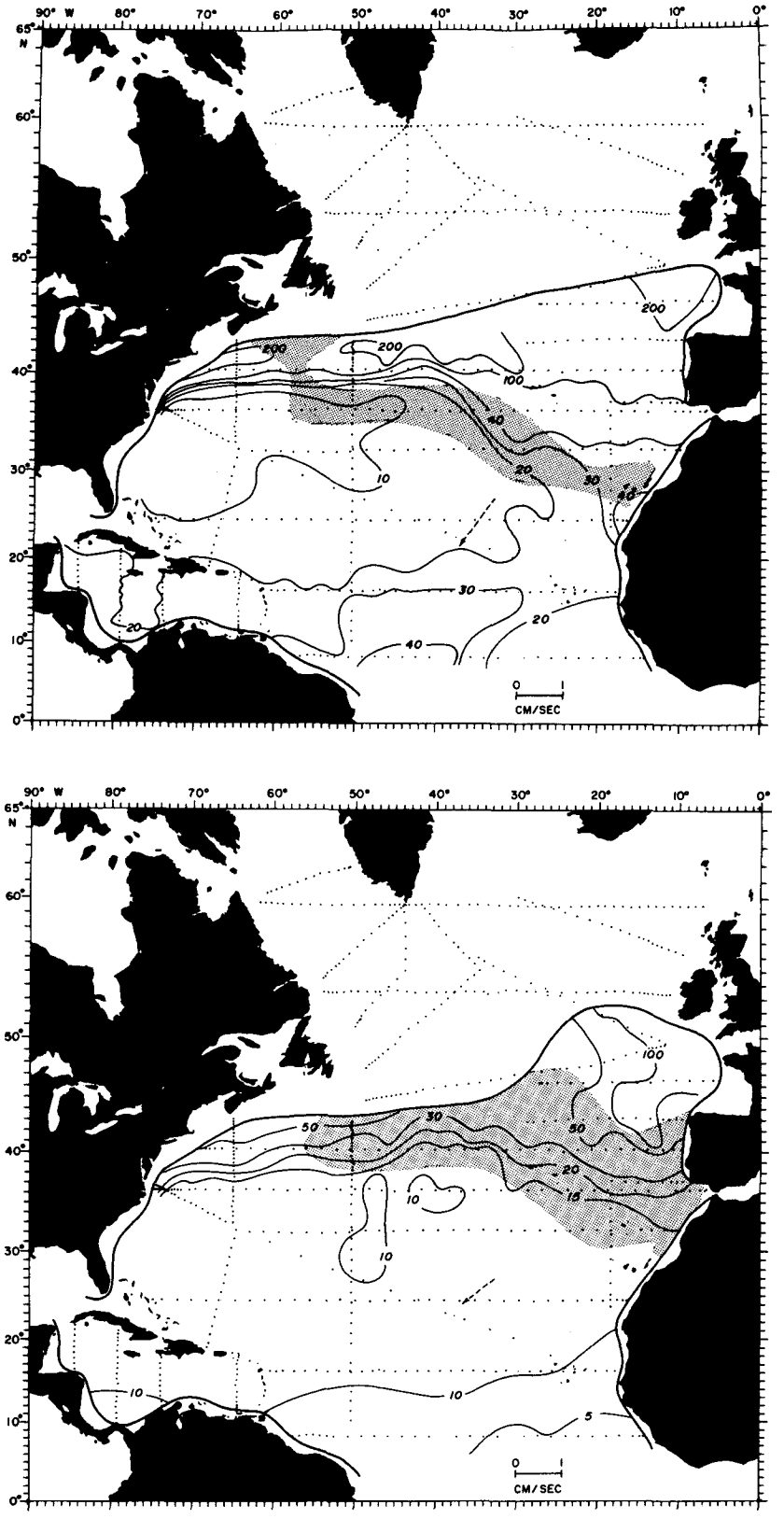

FIG. 1. Potential vorticity fields Q (10^{-11} m^{-1} s^{-1}) from McDowell et al. (1982) for (a) between the $\sigma_\theta = 26.3$ and 26.5 surfaces, the Q contours appear to be closed in the northwest Atlantic, or to be open and thread back to the winter outcrop (shaded area) in the northeast Atlantic, and (b) between the $\sigma_\theta = 26.5$ and 27.0 surfaces, the Q field appears to be relatively homogeneous south of the winter outcrop over most of the subtropical gyre.

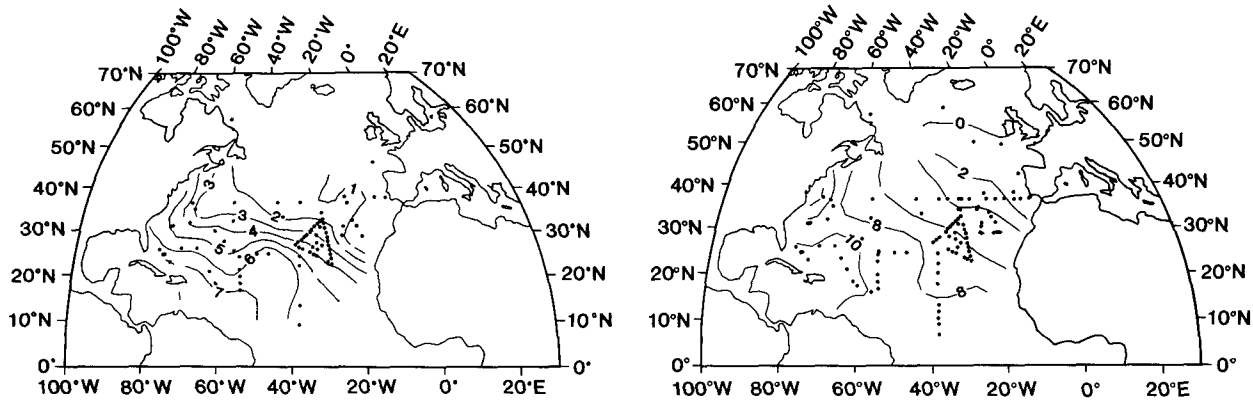

FIG. 2. Observations of the tritium-^{3}He age in years on (a) the $\sigma_\theta = 26.5$ and (b) the $\sigma_\theta = 26.75$ surfaces in the North Atlantic from Jenkins (1988).

thermocline simulation of the North Atlantic by Huang (1990), which concentrates on the flow field in the gyre and uses climatological winter mixed-layer and Ekman pumping fields with the intergyre boundary varying with latitude. Finally, limiting idealized cases are shown in which ventilation can even lead to homogeneous Q occurring throughout the main thermocline (section 5); this limit is also explored in a novel formulation of a thermocline model by Marshall and Nurser (1991).

2. Potential vorticity and the mixed layer

The potential vorticity in the ventilation regime may be defined in terms of fluid leaving the mixed layer and entering the stratified thermocline; see the discussion of Cushman-Roisin (1987) and Williams (1989), which we briefly repeat here. Consider a fluid parcel being swept from a mixed layer of density ρ_m and thickness h into a stratified thermocline by the horizontal $\mathbf{u}_b$ and vertical w_b velocities at the base of the mixed layer (Fig. 3). The vertical spacing Δz between the subducted fluid parcel and the overlying mixed layer increases over a time interval Δt according to the rate of deepening of the parcel, $-w_b$; the rate of mixed-layer shallowing, $-\partial h/\partial t$; and the horizontal advection of the parcel below the shoaling mixed layer, $-\mathbf{u}_b \cdot \nabla h$:

$$S = \frac{\Delta z}{\Delta t} = -\left(w_b + \frac{\partial h}{\partial t} + \mathbf{u}_b \cdot \nabla h \right). \qquad (2)$$

This subduction rate, S, is the volume flux of fluid per unit horizontal area entering the thermocline from the mixed layer.

Assuming that the density is continuous between the mixed layer and the adiabatic thermocline, then the rate of increase in the density difference $\Delta\rho$ between the subducted parcel and the overlying mixed layer depends on the rate of mixed-layer warming, $-\partial\rho_m/\partial t$, and the horizontal advection of the parcel below the warmer mixed layer, $-\mathbf{u}_b \cdot \nabla \rho_m$:

$$\frac{\Delta\rho}{\Delta t} = \frac{\partial \rho_m}{\partial t} + \mathbf{u}_b \cdot \nabla \rho_m. \qquad (3)$$

The potential vorticity of the subducted fluid may, therefore, be defined from (1) to (3) in terms of the planetary vorticity, the velocity at the base of the mixed layer, and the temporal and spatial variations in the mixed-layer fields:

$$Q = \frac{f\left(\dfrac{\partial \rho_m}{\partial t} + \mathbf{u}_b \cdot \nabla \rho_m \right)}{\bar{\rho}\left(w_b + \dfrac{\partial h}{\partial t} + \mathbf{u}_b \cdot \nabla h \right)}. \qquad (4)$$

Subducted fluid acquires a potential vorticity that is (i) *increased* in value through an increase in the rate of mixed-layer warming, $-\partial\rho_m/\partial t$, and cross-isopycnal flow, $-\mathbf{u}_b \cdot \nabla \rho_m$, or is (ii) *decreased* by increasing the

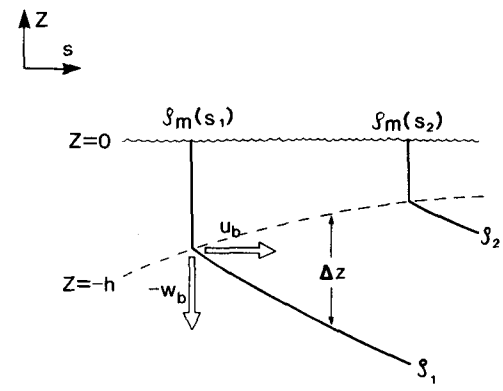

FIG. 3. Schematic diagram showing isopycnals subducted from a mixed layer with a thickness h and density ρ_m; the horizontal coordinate s is aligned parallel to the horizontal flow. The vertical spacing Δz and density difference $\Delta\rho$ between a subducted isopycnal ρ_1 and the mixed layer varies with the vertical w_b and horizontal $\mathbf{u}_b$ velocities at the base of the mixed layer, and the temporal and spatial changes in the mixed-layer depth and density.

subduction rate, S, either through increasing the downward velocity at the base of the mixed layer, $-w_b$, the rate of mixed-layer shallowing, $-\partial h/\partial t$, or the horizontal advection of fluid out of the mixed layer, $-\mathbf{u}_b \cdot \nabla h$.

In this work we incorporate regional variations in the thickness and density of the mixed layer and solve for the potential vorticity and velocity fields in a subtropical gyre using a thermocline model. As the model is steady, we cannot explicitly incorporate the regional variation of the seasonal mixed-layer cycle in (4) (as investigated by Federiuk and Price 1985; Woods and Barkmann 1988; Bleck et al. 1989). This seasonal cycle controls the subduction of fluid into the seasonal thermocline and leads to temporal variability in the main thermocline. In this study we are most interested in the annual mean structure of the main thermocline, and we choose to impose plausible "end of winter" mixed-layer fields, as this is the crucial subduction time when fluid is most likely to enter the main thermocline (Stommel 1979); this is illustrated in the Lagrangian mixed-layer experiments of Cushman-Roisin (1987) and Williams (1989).

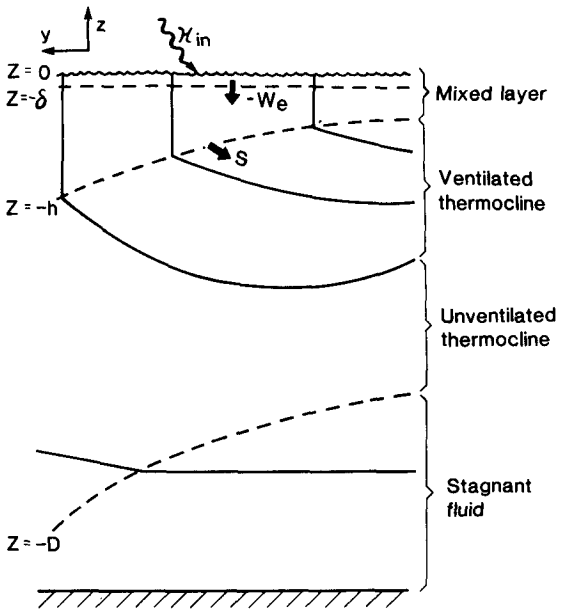

FIG. 4. Schematic north–south section of the thermocline model separated into a shallow Ekman layer ($z = -\delta$), within a deeper mixed layer ($z = -h$), and above a stratified thermocline with moving fluid within the bowl ($z = -D$). The Ekman upwelling w_e and the surface heating $\mathscr{H}_{in}$ drive a cross-isopycnal flow in the mixed layer, leading to fluid being subducted at a rate S into the ventilated thermocline.

3. Ventilation model

The ventilation model follows the continuously stratified thermocline model of Huang (1988), and the extension by Williams (1989) and Huang (1990) to include a mixed layer; the assumptions and formulation are briefly outlined here. The model consists of a shallow Ekman layer embedded within a deeper mixed layer, overlying an adiabatic stratified interior (Fig. 4). The model is forced by Ekman pumping at the base of the Ekman layer, $-w_e$, and implicitly by a surface heat flux, $\mathscr{H}_{in}$, acting over both the Ekman layer and the mixed layer, which is assumed to vertically homogenize the density profile but not the momentum profile. Outside the Ekman layer, the thermocline model assumes steady geostrophic and hydrostatic balance, with the meridional transport satisfying a Sverdrup balance:

$$\int_{-D}^{o} v\,dz = \frac{f}{\beta} w_e. \tag{5}$$

Here D is the depth of the bowl of moving water, v is the meridional geostrophic velocity, and β is the planetary vorticity gradient.

The aim of the ventilation model is to determine the potential vorticity field in the subtropical gyre given appropriate boundary conditions. Ventilated fluid is subducted from the steady mixed layer into the thermocline with its potential vorticity (4) satisfying

$$Q = \frac{f\,\mathbf{u}_b \cdot \nabla \rho_m}{\bar{\rho}(w_b + \mathbf{u}_b \cdot \nabla h)}. \tag{6}$$

In contrast, unventilated fluid enters the thermocline from the western boundary. Its potential vorticity is chosen either to have a homogeneous value, Q_o, if its density surface does not outcrop, or the ventilated value on the western boundary of its outcrop if it does; here $Q_o = 0.1 \times 10^{-9}\ \mathrm{m^{-1}\ s^{-1}}$ and is the reference value along the northern boundary of the subtropical gyre.

Fluid subsequently conserves its potential vorticity in the adiabatic thermocline and follows the geostrophic streamlines on density surfaces—defined by the Montgomery potential, $M = p + \rho g z$, such that

$$\mathbf{u} \cdot \nabla Q = 0$$

with the geostrophic velocity given by

$$\mathbf{u} = \frac{1}{\bar{\rho} f}\,\mathbf{k} \times \nabla M.$$

Here $\mathbf{k}$ is the unit vertical vector and p is the pressure.

The Montgomery potential depends on the vertical position of isopycnals, $Z(\rho)$, through the hydrostatic relation,

$$\frac{\partial M}{\partial \rho} = gZ$$

and hence is related to the potential vorticity (1) by

$$\frac{\partial^2 M}{\partial \rho^2} = -\frac{fg}{\bar{\rho} Q}. \tag{7}$$

Following Huang (1988), the thermocline structure may be determined by integrating (7) for the moving water column and

(i) applying the lower boundary condition of no flow at the base of the bowl with $M(\rho)$ and $Z(\rho)$ having the reference abyssal values $M^a(\rho)$ and $Z^a(\rho)$ at the density of the bowl ρ_d (not imposed),

(ii) determining the $Q(M, \rho)$ of fluid already subducted or unventilated in (7) by threading back upstream along $M(\rho)$ contours to where they intersect the mixed layer or the western boundary,

(iii) satisfying the zonally integrated Sverdrup equation using an imposed Ekman pumping and eastern boundary stratification, $Z_e(\rho, y)$,

$$\int_{\rho_m(x)}^{\rho_d(x)} Z^2 d\rho - \int_{\rho_m(x_e)}^{\rho_d(x)} Z_e^2 d\rho = -\frac{2\bar{\rho} f^2}{\beta g} \int_x^{x_e} w_e dx \quad (8)$$

and

(iv) applying the upper boundary condition of the imposed mixed-layer depth and density, enabling (8) to be solved and allowing the Q of fluid being subducted into the water column to be diagnosed [implicitly satisfying (6)]. This process, (i)–(iv), is then repeated for other grid points covering the entire gyre by systematically moving westward and then southward over the domain.

4. Ventilation model results

a. Sloping mixed layer

The sensitivity of the potential vorticity field in the main thermocline to different mixed-layer fields is examined using a rectangular subtropical gyre on a midlatitude β plane. The gyre extends from 15° to 45°N and 60° to 15°W, with $x = 0$ and x_e on the western and eastern boundaries, and $y = 0$ and y_n on the southern and northern boundaries. The Ekman upwelling is assumed to vary sinusoidally with latitude,

$$w_e(y) = -w_o \sin(\pi y / y_n)$$

with $w_o = 45$ m yr^{-1}.

In order to concentrate on the role of the mixed layer, isopycnals are chosen to be flat along the eastern boundary with the bowl striking the base of the mixed layer here (see Fig. 9a) (following Huang 1990). The potential vorticity of a ventilated isopycnal on its eastern boundary is then solely given in terms of the planetary vorticity and the mixed-layer gradients:

$$Q(x = x_e) = \frac{f}{\bar{\rho}} \frac{\partial \rho_m}{\partial y}\bigg|_{x_e} \Big/ \frac{\partial h}{\partial y}\bigg|_{x_e}. \quad (9)$$

This boundary condition leads to an eastward geostrophic outflow within the mixed layer along the eastern boundary, which we assume is swept away in an eastern boundary current; no attempt is made here to model these higher-order dynamical processes.

We first compare the structure of the ventilated thermocline for a flat and a sloping mixed layer. The flat mixed layer is chosen to have a constant depth of 130 m, whereas the sloping mixed layer is chosen to have the same mean depth and deepen poleward as

$$h(y) = 350 e^{-2.5(1-y/y_n)},$$

which is typical of that observed at the end of winter (Levitus 1982) and is the same as chosen in Pedlosky and Robbins (1991). The mixed-layer density is chosen to outcrop on latitude circles with the $\sigma_\theta = 26.0$, 26.5, and 26.75 positions, typical of the western basin values in the Levitus winter climatology and with $\sigma_\theta = 24.5$ and 27.0 chosen on the southern and northern boundaries, respectively.

The sloping mixed layer modifies the structure of the thermocline by increasing the isopycnal spacing over the gyre compared with the flat case, with isopycnals being subducted at greater depth in the northern

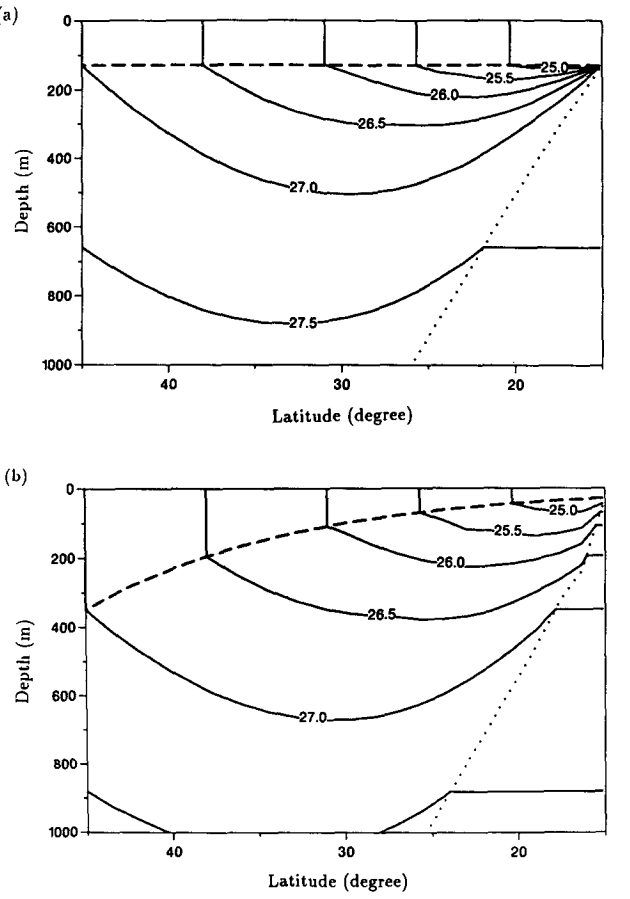

FIG. 5. North–south section along the western edge of the subtropical gyre showing the $\sigma_\theta = 25.0$ to 27.5 surfaces and the depth of the bowl (dotted line) for (a) a flat mixed layer and (b) a sloping mixed layer.

half of the gyre and at shallower depths in the southern half (Fig. 5). Consequently, the subducted fluid acquires a Q that is reduced in magnitude for the sloping case (Fig. 6) with the ventilated values typically ranging from 0.1 to 0.3 ($\times 10^{-9}$ m^{-1} s^{-1}) and now in accord with the magnitude of the observations shown in Fig. 1.

The flat mixed-layer case has a singularity in Q along the eastern and southern boundaries in which all the ventilated isopycnals are artificially compressed together (Fig. 7). This Q singularity leads to a streamline following the eastern and southern boundary. In the sloping case, Q has a finite value on the eastern boundary, which is set by the planetary vorticity and mixed-layer fields in (9) and decreases southward along each isopycnal. On every ventilated surface, this leads to a shadow zone in which the Q contours cannot thread back to the outcrop and so there is no motion.

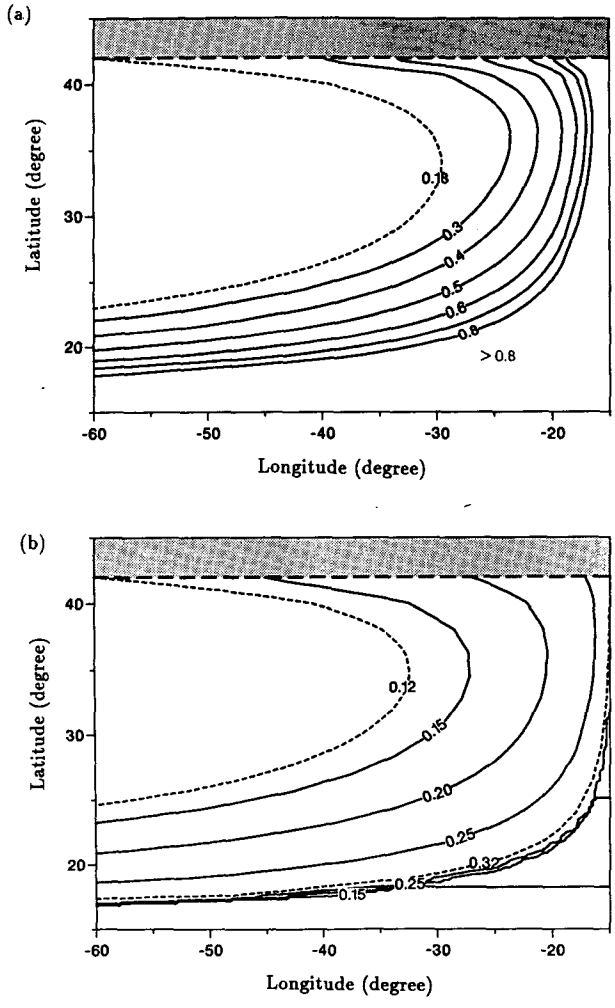

FIG. 6. Subducted potential vorticity field (10^{-9} m^{-1} s^{-1}) along the σ_θ = 26.75 surface for (a) a flat mixed layer and (b) a sloping mixed layer; the outcrop and ventilation zone boundaries are marked by thick and thin dashed lines.

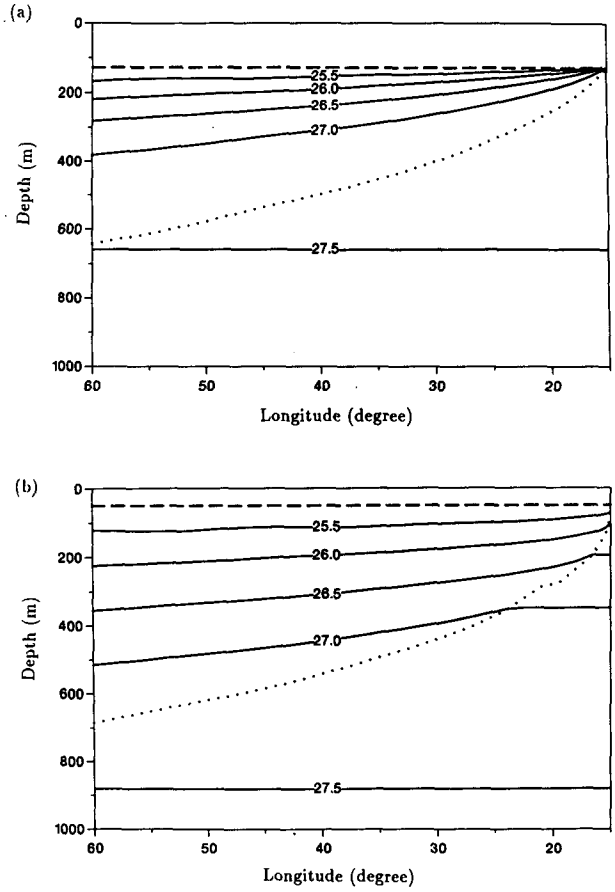

FIG. 7. West–east section along $y = y_n/4$ of the subtropical gyre showing the depth of the σ_θ = 25.5 to 27.5 surfaces and the depth of the bowl (dotted line) for (a) a flat mixed layer and (b) a sloping mixed layer.

The sloping mixed layer modifies the detail of the flow by reducing the value of the subducted potential vorticity and through the emergence of the shadow zone. The flow tends to swing more to the west with the western pool slightly shrinking (Fig. 6), and the weaker flow within the ventilated thermocline leads to the bowl deepening in compensation by typically 50 m in the interior (Fig. 7).

b. *Variable outcrop pattern*

The mixed-layer outcrops are now more realistically allowed to be swept southward by the anticyclonic circulation in the subtropical gyre, rather than be constrained to lie along latitude circles; this tends to occur through mixed-layer advection strengthening as the bowl shoals toward the east (Pedlosky et al. 1984). The outcrop positions on the western and eastern boundaries of the σ_θ = 26.0, 26.5, and 26.75 surfaces are now both chosen to be typical of the Levitus winter climatology with the interior positions varying as

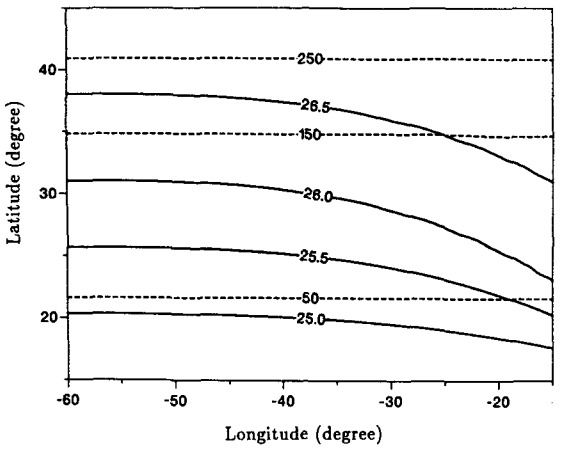

FIG. 8. Mixed-layer σ_θ and depth fields (full and dashed lines) for a sloping mixed layer with a variable outcrop geometry.

$$y(x, \rho_m) = y_w(\rho_m)\left(1 - \frac{x^3}{x_e^3}\right) + y_e(\rho_m)\frac{x^3}{x_e^3}$$

where $y_w(\rho_m)$ and $y_e(\rho_m)$ are the positions on the western and eastern boundaries (Fig. 8).

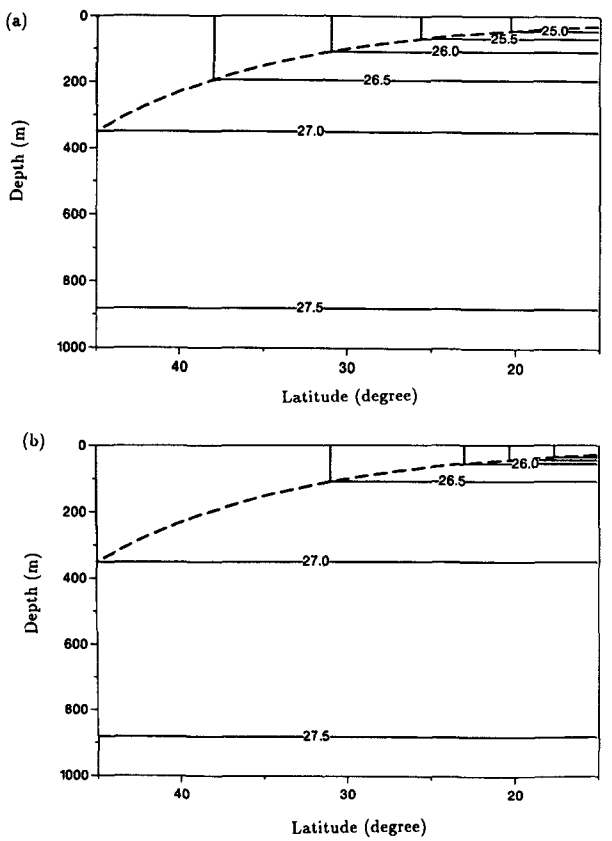

FIG. 9. North-south section along the eastern edge of the subtropical gyre showing the σ_θ = 25.0 to 27.5 surfaces for (a) outcropping on latitude circles and (b) a variable outcrop geometry.

1) POTENTIAL VORTICITY

This more realistic outcrop variation increases the isopycnal spacing and, hence, reduces the Q for $\sigma_\theta \geqslant 26.5$ on the eastern boundary and conversely increases the Q for lighter surfaces, compared with the outcropping along latitude circles case (Fig. 9).

On the σ_θ = 26.4 surface, there are open Q contours threading back to the outcrop with values ranging from 0.13 to 0.5 ($\times 10^{-9}$ m^{-1} s^{-1}) across the gyre (Fig. 10a); whereas on the σ_θ = 26.75 surface, there is a strikingly more uniform Q field with values ranging only from 0.13 to 0.18 ($\times 10^{-9}$ m^{-1} s^{-1}) across the gyre (Fig. 10b).

This appears to be in excellent agreement with the climatological observations in Fig. 1 showing clearly open Q contours on the σ_θ = 26.4 surface and nearly uniform Q on the σ_θ = 26.75 surface.

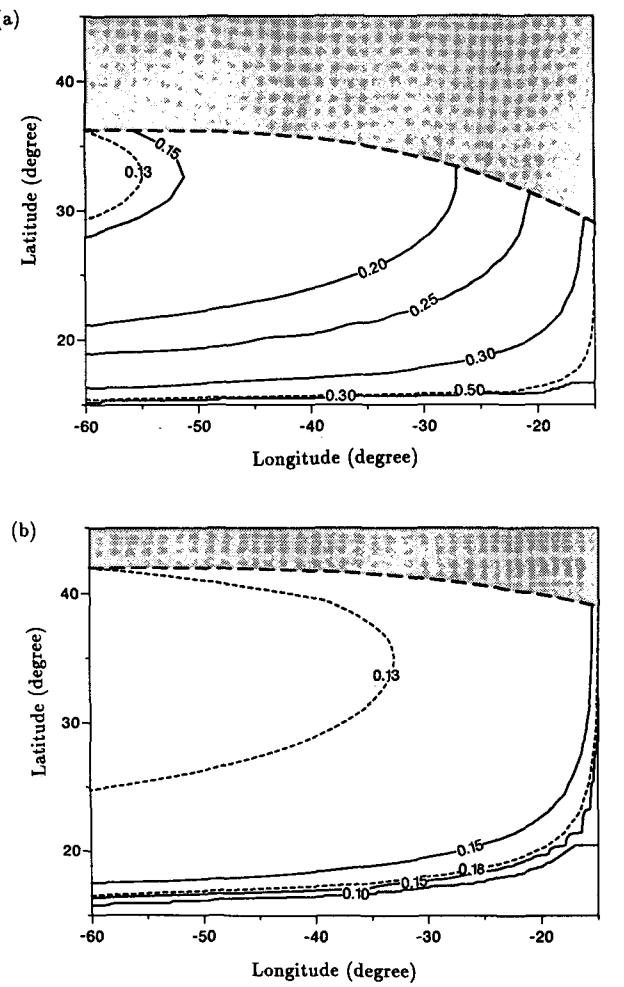

FIG. 10. Subducted potential vorticity field (10^{-9} m^{-1} s^{-1}) along (a) the σ_θ = 26.4 surface and (b) the σ_θ = 26.75 surface for a sloping mixed layer with a variable outcrop geometry; the outcrop and ventilated zone boundaries are marked as thick and thin dashed lines.

2) AGE OF SUBDUCTED FLUID

The age of the subducted fluid varies according to the flow field and the fluid path from the outcrop. The ventilated model shows that the age increases toward the southwest in the gyre as the subducted fluid moves anticyclonically around the gyre and reaches values of typically 6 and 12 years on the western boundary for the $\sigma_\theta = 26.4$ and 26.75 surfaces (Fig. 11). These results are in good agreement with the tritium–helium age observations shown in Fig. 2, which show the corresponding ages reaching 7 and 10 years on the western boundary for the $\sigma_\theta = 26.5$ and 26.75 surfaces. Consequently, this gives further support to the hypothesis that ventilation forms the extensive region of nearly uniform Q on the $\sigma_\theta = 26.75$ surface, with lateral mixing by eddies only being required in the western pool region.

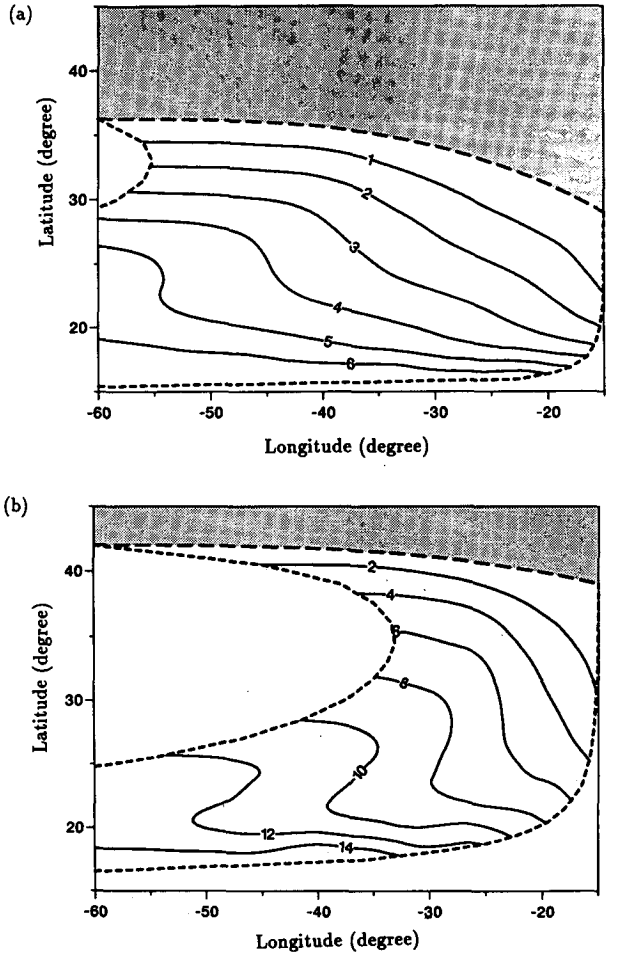

FIG. 11. Age of subducted fluid in years for (a) the $\sigma_\theta = 26.4$ surface and (b) the $\sigma_\theta = 26.75$ surface for a sloping mixed layer with a variable outcrop geometry; the outcrop and ventilated zone boundaries are marked as thick and thin dashed lines.

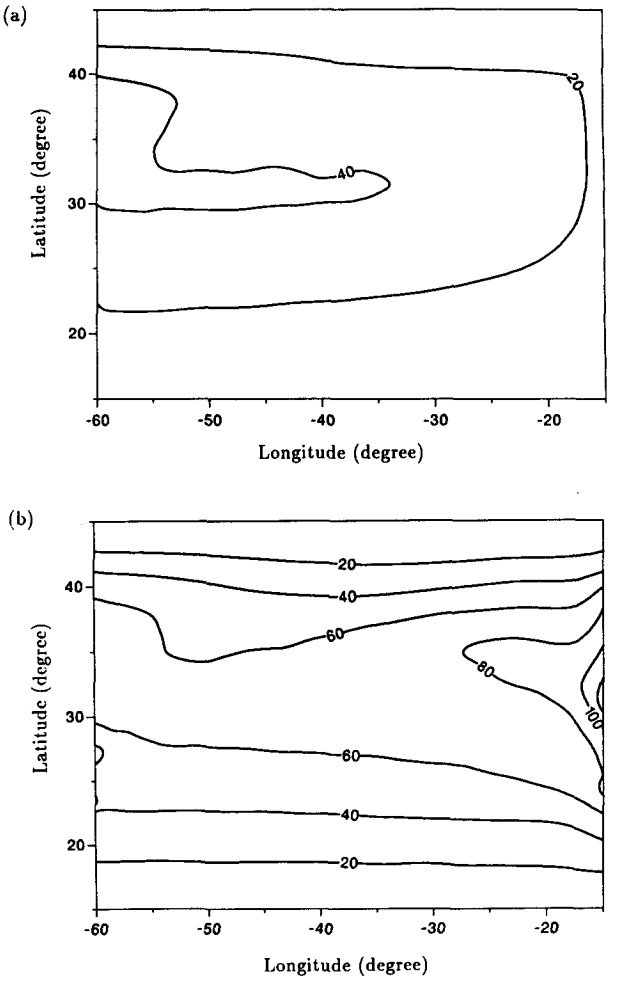

FIG. 12. Subduction rate S (m y^{-1}) in the subtropical gyre for (a) a flat mixed layer and (b) a sloping mixed layer with a variable outcrop geometry.

3) SUBDUCTION RATE

The volume flux of ventilated fluid entering the thermocline layer depends on the vertical and horizontal transfer of fluid from the steady mixed layer (2):

$$S = -(w_b + \mathbf{u}_b \cdot \nabla h). \tag{10}$$

This relation may be written in terms of the Ekman pumping by using (5) to give

$$S = -\left(w_e + \mathbf{u}_b \cdot \nabla h - \frac{\beta}{f}\int_{-h}^{o} v\,dz\right).$$

The subduction rate is enhanced over the Ekman pumping by the lateral transfer of fluid out of the mixed layer, $\mathbf{u}_b \cdot \nabla h$, but is reduced by the meridional transport within the mixed layer, $\int_{-h}^{o} v\,dz$.

In the sloping mixed layer and variable outcrop case, the poleward deepening of the mixed layer increases S up to 80 m yr^{-1}, whereas the flat mixed layer reduces S to only 40 m yr^{-1}, compared with the maximum Ekman pumping of 45 m yr^{-1} (Fig. 12). The longitudinal variation in S is due to the southward mixed-layer flow strengthening as the bowl shoals toward the eastern boundary. The subduction rate then becomes stronger toward the eastern boundary for the sloping mixed layer and conversely weaker for the flat mixed layer.

The increase in S for the sloping mixed layer then leads to the lower value in the subducted Q from (6):

$$Q = -\frac{f\,\mathbf{u}_b \cdot \nabla \rho_m}{\bar{\rho} S}.$$

4) Diabatic forcing

The mixed layer is heated by a surface flux, $\mathscr{H}_{in}$, that balances the cross-isopycnal Ekman, $\mathbf{u}_e$, and geostrophic, $\mathbf{u}_m$, flows within it:

$$\int_{-h}^{o} (\mathbf{u}_e + \mathbf{u}_m) \cdot \nabla \rho_m dz = -\frac{\alpha}{C_w} \mathscr{H}_{in}. \qquad (11)$$

Here α is the density expansion coefficient for temperature, and C_w is the heat capacity for seawater.

The Ekman pumping drives a southward geostrophic flow in the mixed layer over the subtropical gyre, which is enhanced by the horizontal Ekman flow in the northern half of the gyre, but opposed by it in the southern half. Consequently, there is surface heating of the mixed layer over most of the gyre, but with surface cooling near the southern boundary (Fig. 13a).

Nurser and Marshall (1991) connect the subduction rate to a net heating by combining the heat balance of the mixed layer with the potential vorticity relation (6):

$$S = \frac{\alpha f \mathscr{H}_{\text{net}}}{\bar{\rho} C_w h Q}. \qquad (12)$$

Here the net heat flux, $\mathscr{H}_{\text{net}} = \mathscr{H}_{in} - \mathscr{H}_{ek}$, is the surface heat flux minus the heat flux balancing the Ekman transport, $\mathscr{H}_{ek} = (C_w/\alpha\bar{\rho}f)\mathbf{k} \times \tau \cdot \nabla \rho_m$, and τ is the wind stress.

As they emphasize, there is only subduction of fluid into the thermocline when there is a net heating of the mixed layer; this is supported by comparing the S and $\mathscr{H}_{\text{net}}$ fields in Figs. 12b and 13b. The magnitude of S increases with stronger heating, $\mathscr{H}_{\text{net}}$, and decreases with increased values of the mixed-layer depth and the subducted Q.

5) Transport partition of flow

The mixed-layer fields modify the transport partition of the gyre by changing the ventilated proportion of

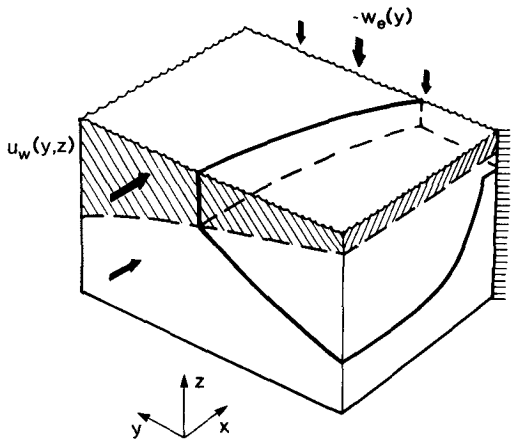

FIG. 14. Schematic diagram showing a mixed layer (hatched region) above the thermocline in the subtropical gyre. Fluid enters the mixed layer either through the Ekman pumping, $-w_e$, or from the zonal inflow, u_w, on the western boundary. This mixed-layer fluid is either subducted into the thermocline or leaves the gyre through the lateral boundaries.

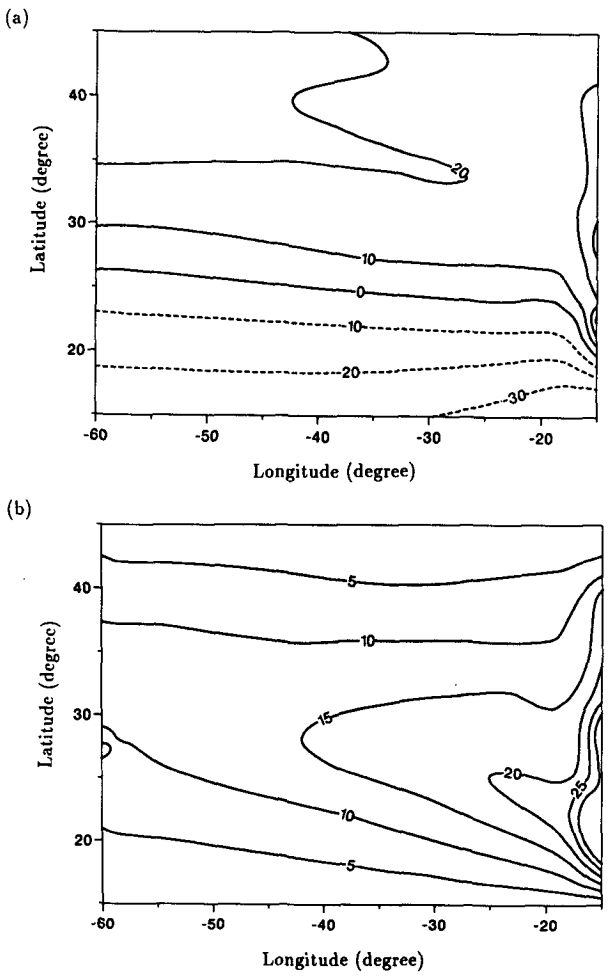

FIG. 13. (a) Surface heat flux $\mathscr{H}_{in}$ and (b) net heat flux $\mathscr{H}_{\text{net}}$ (W m^{-2}) for a sloping mixed layer with a variable outcrop geometry.

the flow (Fig. 14). The wind-stress–curl forcing, fluxes 15 Sv (Sv $\equiv 10^6$ m^3 s^{-1}) of fluid into the subtropical gyre from the Ekman layer and induces the anticyclonic circulation that sweeps 34 Sv into the gyre from the western boundary. Fluid entering the gyre from the Ekman layer, therefore, only makes up $3/10$ of the total volume flux of 49 Sv into the gyre.

Fluid entering the mixed layer makes up a higher proportion of $1/2$ this total volume flux with 10 Sv originating from the western boundary and 15 Sv from the Ekman layer. Most of this volume flux in the mixed layer, 19 Sv, is subducted into the thermocline with the rest leaving the mixed layer via the western and eastern boundaries (4 Sv and 2 Sv, respectively).

In comparison, in the thermocline simulation by Huang (1990), fluid passing through the mixed layer makes up a higher proportion of two-thirds the total volume flux of 52 Sv into the gyre; this is due to the increased lateral flux into the mixed layer from the western boundary and the more realistic subpolar/subtropical gyre boundary that varies with latitude.

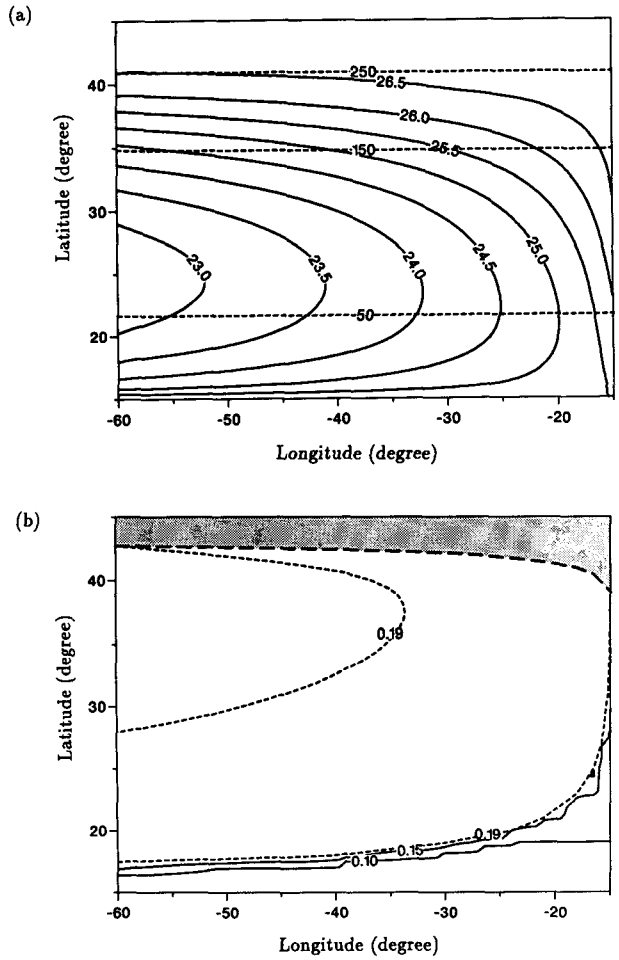

FIG. 15. (a) Mixed-layer σ_θ and depth fields (full and dashed lines) for a mixed layer warming westward and (b) the potential vorticity field (10^{-9} m^{-1} s^{-1}) for $\sigma_\theta = 26.75$; the outcrop and ventilated zone boundaries are marked as thick and thin dashed lines.

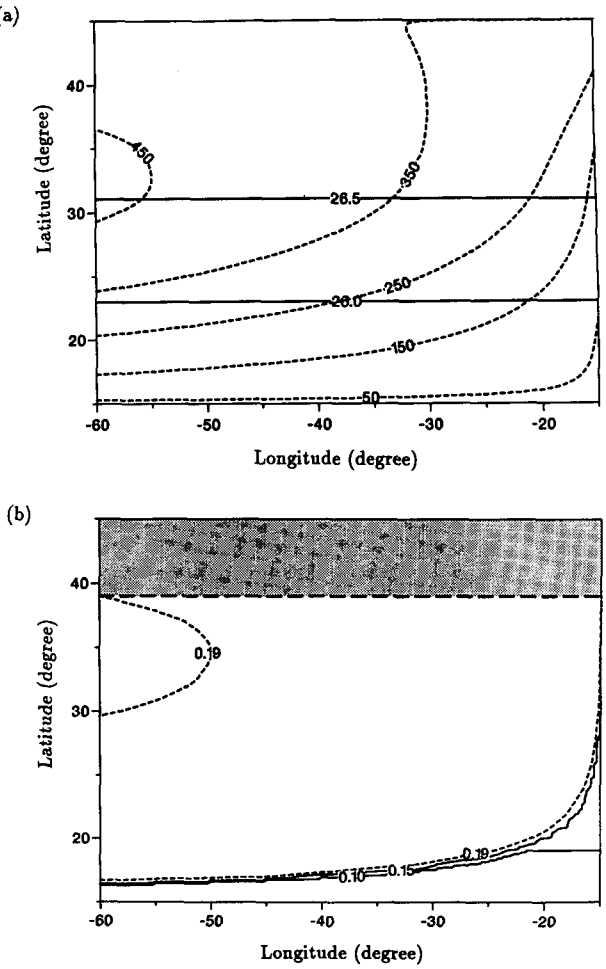

FIG. 16. (a) Mixed-layer density and depth fields (full and dashed lines) for a mixed layer deepening westward and (b) potential vorticity field (10^{-9} m^{-1} s^{-1}) for $\sigma_\theta = 26.75$; the outcrop and ventilated zone boundaries are marked as thick and thin dashed lines.

c. *Homogeneous potential vorticity*

We now extend these variable mixed-layer depth and density cases to show that ventilation may even produce *exactly* homogeneous Q throughout the ventilated thermocline.

In the previous results, the Q distribution is found after imposing the patterns of the Ekman pumping, both the mixed-layer depth and density fields, and the eastern boundary structure. In contrast, we artificially assume that Q is homogeneous on each isopycnal with the same value as on the eastern boundary. The ventilation model is then used to solve for either the mixed-layer density or depth field given the imposed patterns of Ekman pumping, the mixed-layer depth or density field, and the eastern boundary structure. Any venti-

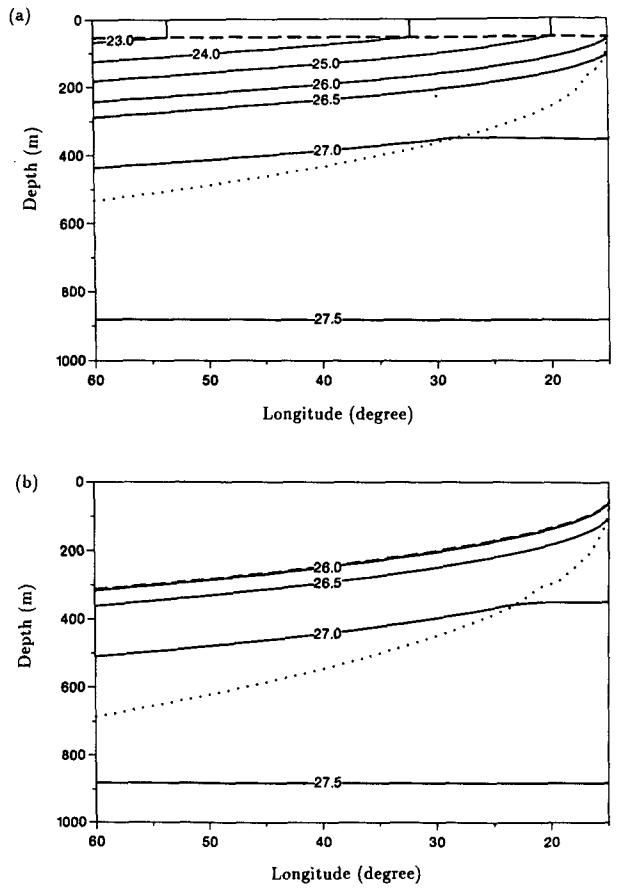

FIG. 17. West–east section along $y = y_n/4$ of the subtropical gyre showing the depth of the σ_θ = 23.0 to 27.5 surfaces and the depth of the bowl (dotted line) for the uniform potential vorticity cases with (a) a mixed layer warming westward and (b) a mixed layer deepening westward.

lated fluid with a lower density than on the southern boundary is chosen to have the same Q as on the southern boundary; so that this large Q does not overdominate the results, the mixed-layer density gradient is reduced here by artificially increasing σ_θ to 25.5 on the southern boundary.

Imposing a mixed layer that only deepens poleward leads to the mixed layer becoming warmer toward the west in order for Q to be uniform along each ventilated surface (Fig. 15). This is clearly an extension of the more realistic variable outcrop case shown in Fig. 8, with the outcrops now orientated even more from the northwest to the southeast; however, the mixed layer is unrealistically warm, and the σ_θ too small over the southern part of the gyre.

Alternatively, requiring that only the mixed-layer outcrop on latitude circles leads to the mixed-layer deepening westward by up to 300 m in order for Q to be uniform along each ventilated surface (Fig. 16). However, the Levitus winter climatology actually shows a slight shoaling of the mixed layer westward, rather than a deepening.

Along a latitude circle, these mixed-layer variations offset the westward deepening of the underlying thermocline induced by Ekman pumping to give a uniform vertical spacing of the isopycnals (Fig. 17). The different mixed-layer fields lead to a different thermocline structure even though the $Q(\rho)$ is the same in both cases. When the mixed layer warms westward, there is a larger southward surface flow, and in compensation, the bowl shoals by up to typically 150 m, compared to when the mixed layer deepens westward.

Ventilation may, therefore, produce an exactly homogeneous Q field through a westward warming or deepening of the mixed layer, but these mixed-layer variations are unrealistically large if this limit is applied over the whole subtropical gyre.

5. Conclusions

The main thermocline is ventilated in the subtropical gyre primarily through fluid being subducted from the winter mixed layer. Ekman pumping drives the anticyclonic circulation that sweeps fluid vertically and laterally from the mixed layer into the thermocline. The subducted fluid acquires a potential vorticity that depends on both mixed-layer density and depth gradients, as well as on the flow pattern and the local planetary vorticity.

The ventilation model shows that incorporating plausible patterns of the winter mixed-layer depth and density leads to the potential vorticity and age fields being in good agreement with observations in the North Atlantic. The study suggests that ventilation forms much of the nearly uniform potential vorticity that is observed on the σ_θ = 26.75 surface, with lateral mixing by eddies only being required in the western pool region.

Observations of nearly uniform potential vorticity, therefore, do not necessarily identify which process is responsible for forming them. Other tracers must also be used to indicate whether properties on isopycnals are being smeared out by the eddy field or whether they are advected into the gyre from the winter mixed layer.

Acknowledgments. This work was supported by the Natural Environment Research Council of the United Kingdom. I am grateful to John Marshall and George Nurser for helpful discussions.

REFERENCES

Bleck, R., H. P. Hanson, D. Hu, and E. B. Kraus, 1989: Mixed layer—thermocline interaction in a three-dimensional isopycnic coordinate model. *J. Phys. Oceanogr.*, **19**, 1417–1439.

Cushman-Roisin, B., 1987: Dynamics of the oceanic surface mixed layer. Hawaii Institute of Geophysics Special Publications, P. Muller and D. Henderson, Eds., 181–196.

Federiuk, J. M., and J. F. Price, 1985: Mechanisms of oceanic subduction, unpublished manuscript.

Huang, R. X., 1988: On boundary value problems of the ideal-fluid thermocline. *J. Phys. Oceanogr.*, **18,** 619–641.

——, 1990: On the three-dimensional structure of the wind-driven circulation in the North Atlantic. *Dyn. Atmos. Oceans,* **15,** 117–159.

Jenkins, W. J., 1988: The use of anthropogenic tritium and helium-3 to study subtropical gyre ventilation and circulation. *Phil. Trans. R. Soc. London,* **A 325,** 43–61.

Keffer, T., 1985: The ventilation of the World's Oceans: Maps of the potential vorticity field. *J. Phys. Oceanogr.*, **15,** 509–523.

Levitus, S., 1982: Climatological atlas of the World Ocean. NOAA Prof. Pap. 13, Washington D.C., 173 pp.

Luyten, J. R., J. Pedlosky, and H. Stommel, 1983: The ventilated thermocline. *J. Phys. Oceanogr.*, **13,** 292–309.

Marshall, J. C., and G. Nurser, 1986: Steady free circulation in a quasigeostrophic ocean. *J. Phys. Oceanogr.*, **16,** 1799–1813.

——, and A. J. G. Nurser, 1991: A continuously stratified thermocline model incorporating a mixed layer of variable depth and density. *J. Phys. Oceanogr.*, **21,** 1780–1792.

McDowell, S., P. B. Rhines, and T. Keffer, 1982: North Atlantic potential vorticity and its relation to the general circulation. *J. Phys. Oceanogr.*, **12,** 1417–1436.

Nurser, A. J. G., and J. C. Marshall, 1991: On the relationship between subduction rates and diabatic forcing of the mixed layer. *J. Phys. Oceanogr.*, **21,** 1793–1802.

Pedlosky, J., and P. Robbins, 1991: The role of finite mixed-layer thickness in the structure of the ventilated thermocline. *J. Phys. Oceanogr.*, **21,** 1018–1031.

——, W. Smith, and J. R. Luyten, 1984: On the dynamics of the coupled mixed-layer-thermocline system and the determination of the oceanic surface density. *J. Phys. Oceanogr.*, **14,** 1159–1171.

Rhines, P. B., and W. R. Young, 1982: A theory of the wind-driven circulation. I. Mid-ocean gyres. *J. Mar. Res.*, **40**(Suppl.), 559–596.

Stammer, D., and J. D. Woods, 1987: Isopycnic potential vorticity atlas of the North Atlantic Ocean—monthly mean maps. *Ber. Inst. Meereskd. Univ. Kiel,* **165,** 108.

Stommel, H., 1979: Determination of watermass properties of water pumped down from the Ekman layer to the geostrophic flow below. *Proc. Natl. Acad. Sci., U.S.A.*, **76,** 3051–3055.

Williams, R. G., 1989: Influence of air–sea interaction on the ventilated thermocline. *J. Phys. Oceanogr.*, **9,** 1255–1267.

Woods, J. D., 1985: Physics of thermocline ventilation. *Coupled Atmosphere–Ocean Models.* J. C. J. Nihoul, Ed., Elsevier, 543–590.

——, and W. Barkmann, 1988: A Lagrangian mixed-layer model of Atlantic 18°C water formation. *Nature,* **319,** 574–576.